

Nanomagnetism and Polarized Neutrons

F. Klose

ANSTO, Bragg Institute, PMB 1, Menai NSW 2234, Australia.

This article discusses current trends in magnetic thin film and spintronic research and the applicability of polarized neutron scattering in regard to these artificially layered materials. The capabilities of ANSTO's new polarized beam reflectometer *Platypus* are also briefly outlined.

1. Current Trends in Magnetic Thin Film and Spintronic Research

Presently, electronic technologies are largely dominated by semiconductor based devices in which the charge of the electron is used for processing, storing and retrieving of information. Processor and Random Access Memory chips in computers are examples of fast and cost effective devices. However, in order to keep up with the increasing requirements for further miniaturization, higher speed and lower power consumption of devices, novel scientific solutions for fast, reliable and energy efficient processing and storing of data must be developed.

In this regard, spintronics (or spin electronics) is a very promising approach [1,2]. Spintronic devices specifically exploit the spin properties of the electrons (i.e. its magnetism) instead of or in addition to charge degrees of freedom. Magnetism-dependent spin transport in metals and semiconductors, for example, is not only of fundamental research interest, but already has demonstrated its usefulness in electronics applications. The prototype device that is already in use in industry, for example as a read head in hard disk drives and as a memory-storage cell, is the giant-magnetoresistive (GMR) sandwich structure which consists of alternating ferromagnetic and nonmagnetic metal layers (the 2007 Nobel price was awarded to Peter Gruenberg and Albert Fert for this discovery [3]). Depending on the relative orientation of the magnetizations in magnetic layers, the device resistance changes from small (parallel magnetizations) to large (antiparallel magnetizations). The resistance change can exceed 10% at room temperature. This change in resistance (also called magnetoresistance) can be used to sense very small changes in magnetic fields (for example the dipole field of a magnetic bit stored on a hard disk drive).

Recent efforts in improving GMR technology have also involved magnetic tunnel junction (MTJ) devices where the tunneling current through a non-conducting spacer layer depends on the magnetic orientations of its electrodes [4]. The observed magnetoresistivity effect in MTJs can be as large as 1000%, i.e. over an order of magnitude larger than the highest observed values for GMR structures with metallic spacer layers. Magnetic tunnel junctions are the essential building blocks for a new type of memory device, the MRAM (magnetic random access memory) [1]. A MRAM is in principle an array of magnetic tunnel junctions, where each of the MTJs represents one bit of stored information (depending on the relative orientation of the upper and lower magnetic electrodes, the MTJ is either in "high" or "low" resistance state). The MTJs are connected to an electronic circuit via an array of metallic lines which allows reading of individual MTJs as well as writing by changing the relative magnetic orientation of the MTJ's electrodes. The first MRAM chip was commercially available in 2006 [5]. The main advantages of the MRAM compared to a Si based RAM device are the non-volatility of the stored information and the resulting low power consumption.

Multiferroics are another class of materials which potentially could have applications in spintronic devices [6]. Multiferroics are materials that simultaneously have *ferroelectric* and *ferromagnetic* properties. Ferroelectric and ferromagnetic materials are similar in many ways, belonging to a broader family called ferroics. Both material classes show features such as a spontaneous moment (dipole vs. electron spin), sensitivity to applied bias (electric vs. magnetic), complex domain structures and finally strain effects under an applied bias (electrostriction/piezoelectricity vs. magnetostriction). Both types of materials have been used for traditional functional applications such as storage memory media, sensors and actuators. There has been tremendous interest in designing systems which are “multiferroic”, i.e. materials that possess both ferroelectric and ferromagnetic properties. Such materials could offer the intriguing possibility to control electron spin polarization, ferroelectric lattice polarization and stress through cross-coupled effects. The key idea for device applications is the possibility to control magnetic properties (for example the direction of a magnetic bit) by applying electric fields across the material or, vice versa, to control the flow of current by externally controlling the magnetization of the same material. Spintronic applications of multiferroic materials, due to the necessary miniaturization and for cost reasons, will require multiferroic materials in thin film form. Since bulk multiferroic materials are extremely rare anyway, thin film hybrid structures (made by interfacing ferroelectric and ferromagnetic materials) are believed to have enormous potential for exciting research and applications.

2. Polarized Neutron Reflectometry

Polarized neutron reflectometry (PNR) has a successful track record of providing unique insights in problems of magnetic surfaces, thin films, interfaces, and multilayer systems (for recent reviews, see [7,8]). Areas of current fundamental science addressed by this technique include flux penetration and flux-lattice ordering in superconductors, nucleation and growth of structured surfaces, magnetic moment formation in thin films, interface polarization, interfacial coupling and quantum confinement, giant/tunneling and colossal magnetoresistance. In the future, investigations on magnetic domains and patterned structures of magnetic dots or other nanoparticles, self-assembled layers and integrated materials such as polymers combined with magnetic materials, molecular magnets etc. will become increasingly important. Fundamentally new scientific insights gained by PNR were and will be important in the development of future thin-film based applications, such as new hard and soft magnetic materials to improve the efficiency of energy delivery systems (e.g., motors, transformers, etc.), magnetic recording media and magnetic sensors for computers, new magnetic memory technologies such as non-volatile magnetic random access memory (MRAM) and other *spintronics* devices.

Next generation neutron scattering instruments with much higher available neutron flux such as the *Magnetism Reflectometer* at the Spallation Neutron Source, USA or the *Platypus* reflectometer at ANSTO, Australia [9] will provide unprecedented experimental capabilities. Most importantly, they will be capable of routinely detecting weak off-specular scattering signals resulting from chemical/magnetic structures *within* the layer plane using off-specular / grazing-incidence small-angle scattering (GISANS) techniques [10,11]. Such experiments are unreasonably slow on today's instruments. These reflectometers will be capable of directly detecting scattering signals of a few monolayers of atoms. The high neutron flux will make possible in-situ structural or magnetic phase-diagram determinations as functions of thermodynamic parameters such as temperature, pressure, atmosphere, magnetic field, etc. and will even provide the ability for time-dependent studies by triggering the data acquisition system with pulsed magnetic, electric, light or other fields.

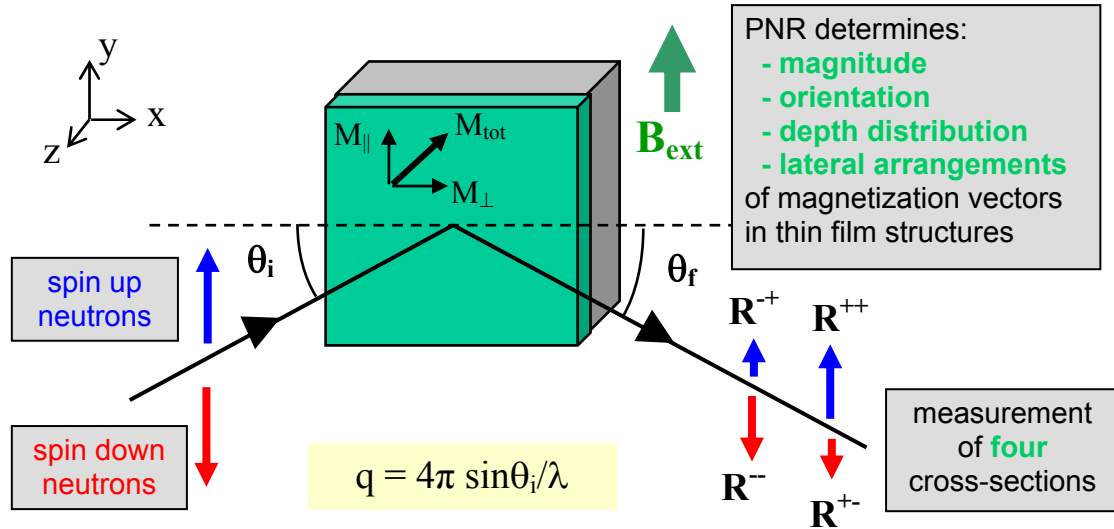


Fig. 1. Schematic representation of the scattering geometry in polarized neutron reflectometry experiments (see text). The thin film sample (green color) is usually deposited on a substrate material (grey). The magnetic moment vector \mathbf{M}_{tot} may have components parallel and perpendicular to the neutron polarization axis.

Figure 1 schematically displays the scattering geometry in PNR experiments. Note that a similar geometry also applies for general diffraction experiments with polarization analysis. A peculiarity of the thin film case is that the shape anisotropy usually forces the magnetic moments to lie within the plane of the surface. The lateral arrangement of the moments, however, is generally determined by other causes, for example resulting from crystalline anisotropies or exchange coupling energies. Therefore, in PNR experiments, magnetic fields \mathbf{B}_{ext} are typically applied within the sample plane (e.g. along the y axis in Fig. 1). The direction of \mathbf{B}_{ext} also defines the polarization axis of the neutron beam. In polarized reflectometry experiments, one measures four different cross-sections as functions of the scattering vector \mathbf{q} . The scattering vector can be scanned in two different ways: reactor type instruments typically use monochromatized neutrons and vary the scattering angle, while pulsed neutron beam instruments (like ANSTO's Platypus) use the time-of-flight method at a fixed angle of incidence to scan λ and consequently \mathbf{q} . R^{++} and R^{-} are the *non-spin flip* reflectivities (the first superscript characterizes the incident neutron polarization and the second the exit polarization; + corresponds to “spin up”, – to “spin down”, respectively). These cross-sections are sensitive to the chemical layering of the film structure as well as the magnetic moment component \mathbf{M}_{\parallel} that is oriented *parallel* to the neutron polarization axis. Provided that no other causes are present that lead to spin-flip scattering, R^{+-} and R^{-+} are sensitive to magnetic moment components \mathbf{M}_{\perp} that are *perpendicular* to the neutron polarization axis. Therefore, PNR reveals not only the depth profile of collinear magnetic structures, but also allows studies of non-collinear magnetic arrangements, including chiral structures.

Provided that the substrate is sufficiently flat and the film is laterally homogeneous, the scattering is *specular*, i.e. the angle of incidence θ_i equals the take-off angle θ_f . In this case, reflectometry measures the chemical and magnetic depth profile along the z axis. In the first order Born approximation, the scattered intensity is given by

$$I(q_z) \propto \frac{1}{q_z^4} \left| \int \frac{dV(z)}{dz} \exp(-iq_z z) dz \right|^2$$

where $V(z)$ is the potential that the neutron experiences at a depth z inside the film [12]. This means that the specular intensity is proportional to the square of the Fourier transformation of the gradient of the potential profile perpendicular to the surface. For a homogeneous layer consisting of a pure element, and with all its magnetic moments aligned parallel to \mathbf{B}_{ext} , $V(z)$ is constant throughout its depth and is given by

$$V = \frac{2\pi\hbar n}{m_n}(b \pm p)$$

In this expression, m_n is the neutron mass, n is the number density and b (p) is the nuclear (magnetic) scattering length of the atom species, respectively. For spin up neutrons, the magnetic contribution p has to be added to b , while for spin down neutrons it has to be subtracted. For this particular case of aligned magnetic moments only R^{++} and R^- will have intensity. Since no perpendicular components of magnetic moments are present, no spin-flip scattering will occur and $R^+ = R^{+-} = 0$. Note that, in contrast to the diffraction regime, reflectivity is measured at low momentum transfer and, therefore, $V(z)$ is a locally averaged potential. In the case that the material consists of different atomic species, their individual contributions to the average local potential have to be summed up. For a sequence of layers, $V(z)$ changes continuously along the depth of the film.

It is well known that the Born approximation fails for $q_z \rightarrow 0$ (the intensity would become infinite at $q_z = 0$). In this regime, optical methods need to be applied that correspond to full dynamical theory taking multiple scattering, refraction and absorption effects into account. A particularly useful method is the recursion scheme of Parratt [13]. This method does not contain approximations and provides exact solutions for reflectivity profiles. Interface roughness can be simulated by slicing the interface region in arbitrarily small regions that approximate the gradient of the potential.

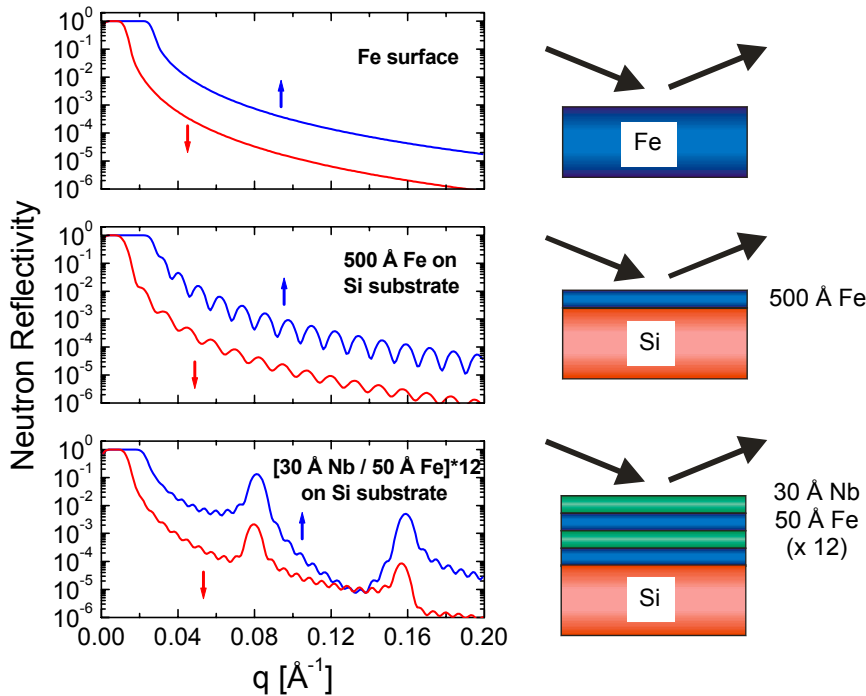


Fig. 2. Calculated PNR spectra for different layer sequences. Upper data set: a bulk Fe surface; middle: a 500 Å Fe film on Si substrate; bottom: a multilayer consisting of 30 Å Nb / 50 Å Fe with 12 repetitions on Si substrate. In all cases it is assumed that the magnetic layers are saturated along the magnetic guide field B_{ext} . R^{++} is plotted in blue and R^- in red color.

Figure 2 displays calculated PNR spectra of typical thin film structures. For all film structures, the region of total reflection and the overall intensity is different for the R^{++} and R^- cross sections. While the reflectivity functions of the Fe surface are featureless declining proportional to $1/q^4$, the interference between partial waves reflected by the vacuum/film and film/substrate interfaces causes an oscillatory behavior of the reflectivity for the 500 Å Fe film (*Kiessig fringes*). The main feature of the multilayer reflectivity function is that strong Bragg peaks occur, which result from the 80 Å double-layer thickness (50 Å Fe + 30 Å Nb).

As mentioned above, laterally structured magnetic films are becoming an increasingly more important research topic. Recently developed polarized *off-specular* / *diffuse* scattering methods allow investigations of lateral (in-plane) magnetic correlations and magnetization fluctuations on length-scales between 1 nm and 100 μm. Analyzing such scattering patterns reveals information on size, shape and periodicity of these nanostructures as well as depth-resolution [14,15]. Of course, this is particularly useful if the surface pattern is not known from the outset, for example in the case of self-assembled structures. In order to extract magnetic information, the use of polarized neutrons and polarization analysis is essential. The method allows, for example, determining details of the magnetization reversal process, and in particular, it permits distinguishing between domain reversal by a rotation or along a particular axis along the surface [16].

If the lateral length scale of the surface structure is large compared to the lateral coherence length of the neutron beam (the latter is typically on the order of microns to tens of microns), there is practically no off-specular intensity and no information on the size of lateral structure is available. Nevertheless, polarized neutron *specular* reflections may contain information on the lateral arrangements of large-scale magnetization inhomogeneities, such as large domains. Lee et al. recently measured the field-dependence of the ferromagnetic domain dispersion of an exchange biased CoO/Co bilayer film and demonstrated the possibility to extract information on the lateral distribution of magnetic domain orientations [17].

3. Outlook on ANSTO's Platypus Reflectometer

The *Platypus* reflectometer [9,18] is part of the initial suite of neutron scattering instruments which started commissioning experiments at the new OPAL reactor at ANSTO in 2007. Despite OPAL being a continuous neutron source, *Platypus* uses a pulsed operation mode, i.e. a chopper system creates bursts of polychromatic neutrons whose wavelengths are sorted out at the detector using the time-of-flight technique (see above). The chopper repetition frequency f depends on the desired neutron wavelength bandwidth $\Delta\lambda = \lambda_{\max} - \lambda_{\min}$ and the distance D from chopper to detector (a typical parameter set is $f = 27.5$ Hz, $\Delta\lambda = 20$ Å and $D = 9$ m). *Platypus*'s neutron beam is produced by a cryogenically cooled deuterium moderator. The guide system which transports the neutrons from the moderator to the beamline is designed to be effective for $\lambda > 2$ Å, i.e. for "cold" neutrons. The white beam flux on the sample is predicted to be as high as 3×10^9 neutrons/cm²/s (by polarizing the beam, the intensity typically drops to 1/3 of this value). Neutrons scattered by the sample (a typical sample size is 25 mm x 25 mm) are detected by a ³He area detector (size: 250 mm x 500 mm; spatial resolution: about 2.5 mm). The beam polarization will be achieved by using Fe/Si supermirror transmission polarizers with very large critical angle ($m = 3.8$) and the specularly reflected beam will be polarization analyzed by a similar device. A spin filter based on polarized ³He gas will allow measuring off-specular/diffuse scattering samples. Radio-frequency spin flippers will allow reversing the beam polarization state before and after the sample. Magnetic fields up to 5 T will be available at the sample position.

In summary, the expected performance of *Platypus* will be well competitive with the best reflectometers in the world and it will enable leading edge science for the Australian neutron scattering community.

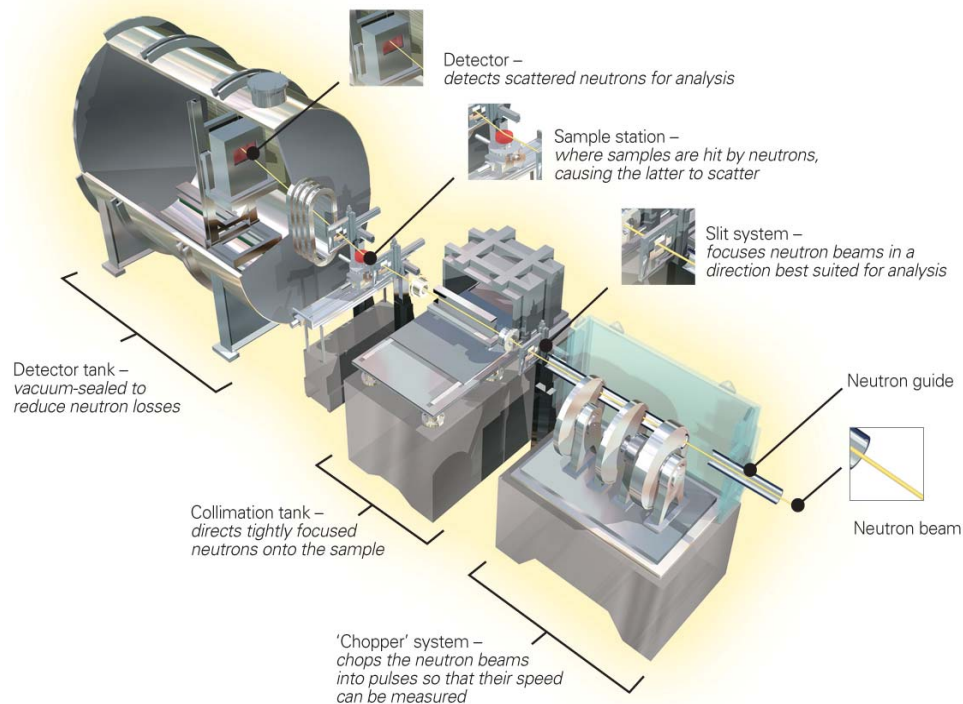


Fig. 3. Platypus, the new time-of-flight polarized beam reflectometer at ANSTO (schematic).

References

- [1] S. Parkin, X. Jiang, C. Kaiser, A. Panchula, K. Roche, M. Samant, *Proceedings of the IEEE* **91**(5), 661 (2003).
- [2] C. Chappert, A. Fert and F.N. Van Dau, *Nature Materials* **6**, 813 (2007).
- [3] see http://nobelprize.org/nobel_prizes/physics/laureates/2007/index.html
- [4] W.H. Butler and A. Gupta, *Nature Materials* **3**, 843 (2004) and references therein.
- [5] see <http://www.freescale.com/>
- [6] R. Ramesh and N.A. Spaldin, *Nature Materials* **6**, 21 (2007).
- [7] H. Zabel, *Materials Today* **9** (1-2), 42 (2006).
- [8] M.R. Fitzsimmons et al., *J. Magn. Magn. Mater.* **271**, 103 (2004).
- [9] M. James, A. Nelson, A. Brule and J. C. Schulz, *Journal of Neutron Research*, **14**, 91 (2006).
- [10] P. Mueller-Buschbaum, J.S. Gutmann, R. Cubitt, M. Stamm, *Colloid Polym. Sci.* **277**, 1193 (1999).
- [11] G.P. Felcher, and S.G.E. te Velthuis, *Appl. Surf. Sci.* **182**, 209 (2001)
- [12] J. Als Nielsen, in *Topics in Current Physics. Structure and Dynamics of Surfaces* (Springer, Berlin, 1986).
- [13] L.G. Parratt, *Phys. Rev.* **95**, 359 (1954).
- [14] B.P. Toperverg, *Physica B* **297**, 160 (2001).
- [15] W.-T. Lee, F. Klose, H.Q. Yin, and B. Toperverg, *Physica B* **335**, 77 (2003).
- [16] K. Temst, M.J. Van Bael, and H. Fritzsche, *Appl. Phys. Lett.* **79**, 991 (2001).
- [17] W.T. Lee, S. G. E. te Velthuis, G. P. Felcher, F. Klose, T. Gredig, D. Dahlberg, *Phys. Rev. B* **65**, 224417 (2002).
- [18] see <http://www.ansto.gov.au/bragg/facilities/instruments/platypus>